Published in final edited form as:
Mol Cancer Ther. 2014 August ; 13(8): 2050–2061. doi:10.1158/1535-7163.MCT-13-1063.

FAK inhibition disrupts a β5 integrin signaling axis controlling anchorage-independent ovarian carcinoma growth

Isabelle Tancioni, **Sean Uryu**, **Florian J. Sulzmaier**, **Nina R. Shah**, **Christine Lawson**, **Nichol L.G. Miller**, **Christine Jean**, **Xiao Lei Chen**, **Kristy K. Ward**, and **David D. Schlaepfer**[1]
Department of Reproductive Medicine, UCSD Moores Cancer Center, La Jolla, CA 92093

Abstract

Ovarian cancer ascites fluid contains matrix proteins that can impact tumor growth via integrin receptor binding. In human ovarian tumor tissue arrays, we find that activation of the cytoplasmic focal adhesion (FAK) tyrosine kinase parallels increased tumor stage, β5 integrin, and osteopontin (OPN) matrix staining. Elevated OPN, β5 integrin, and FAK mRNA levels are associated with decreased serous ovarian cancer patient survival. FAK remains active within ovarian cancer cells grown as spheroids, and anchorage-independent growth analyses of seven ovarian carcinoma cell lines identified sensitive (HEY, OVCAR8) and resistant (SKOV3-IP, OVCAR10) cells to 0.1 μM FAK inhibitor (VS-4718, formerly PND-1186) treatment. VS-4718 promoted HEY and OVCAR8 G0/G1 cell cycle arrest followed by cell death whereas growth of SKOV3-IP and OVCAR10 cells were resistant to 1.0 μM VS-4718. In HEY cells, genetic or pharmacological FAK inhibition prevented tumor growth in mice with corresponding reductions in β5 integrin and OPN expression. β5 knockdown reduced HEY cell growth in soft agar, tumor growth in mice, and both FAK Y397 phosphorylation and OPN expression in spheroids. FAK inhibitor resistant (SKOV3-IP, OVCAR10) cells exhibited anchorage-independent Akt S473 phosphorylation and expression of membrane-targeted and active Akt in sensitive cells (HEY, OVCAR8) increased growth but did not create a FAK inhibitor resistant phenotype. These results link OPN, β5 integrin, and FAK in promoting ovarian tumor progression.β5 integrin expression may serve as a biomarker for serous ovarian carcinoma cells that possess active FAK signaling.

Keywords

ovarian cancer; focal adhesion kinase; spheroids; β5 integrin; osteopontin

Introduction

Ovarian cancer is the 5th leading cause of cancer death in women in the U.S. (1). Initial tumor spread is by an exfoliative mechanism whereby cells dissociate from a primary site and can proliferate in an anchorage-independent manner as clumps of aggregated cells

[1]Address correspondence to: David D. Schlaepfer, Ph.D., University of California San Diego, Moores Cancer Center, Department of Reproductive Medicine, 0803, 3855 Health Sciences Dr., La Jolla, CA 92093, dschlaepfer@ucsd.edu.

Conflicts of Interest
The authors have no conflicts of interest to disclose.

termed spheroids within the peritoneal space (2). Anchorage-independent growth is a hallmark of cell transformation and is connected to elevated tumorigenic potential (3).

In addition to being a sign of advanced disease, ascites contains growth factors and soluble matrix proteins that can enhance ovarian spheroid growth (4). Matrix proteins such as fibronectin, vitronectin, and osteopontin (OPN) are ligands for integrin receptors and are present in high levels within ascites (5). OPN is also a potential diagnostic blood biomarker for ovarian cancer (6, 7). Matrix proteins can become integrated within tumor spheroids to provide a structural scaffold as well as promote signals regulating tumor growth and survival (8, 9). Transmembrane integrin receptors bind matrix proteins and integrin α5β1 binding to fibronectin is linked to ovarian tumor metastasis in mouse models (10). However, clinical trials of an anti-α5β1 antibody did not show activity as a single agent in platinum-resistant ovarian cancer patients (11). This may be due to signals from multiple β-integrin receptors for various matrix proteins that may require co-inhibition to prevent refractory ovarian tumor growth *in vivo*.

Integrin β integrin subunits activate a common set of cytoplasmic tyrosine kinases and targeting this proximal linkage may be an effective means to block signals from multiple integrin receptors (12). The cytoplasmic focal adhesion (FAK) tyrosine kinase is recruited and activated by β1, β3, and β5 integrin subunits. These β integrins can pair with the αv integrin subunit, and together, signals are generated that modulate tumor survival and growth (13). FAK gene amplification occurs in ~24% of serous ovarian cancer and elevated FAK mRNA levels are associated with decreased overall patient survival (12). Although canonically known as a cell adhesion-activated kinase, FAK inhibition does not prevent the proliferation of cells normally cultured on plastic (14, 15). However, increased tumor apoptosis occurs upon pharmacological FAK inhibition in mouse xenograft tumor models (16–18) and sub-micromolar concentrations can trigger apoptosis of tumor cell lines when cultured under anchorage-independent conditions (12, 19). Completed Phase I trials of PF-00562271 FAK inhibitor revealed a subset of patients with stable disease (20), but molecular mechanisms driving tumor cell sensitivity or resistance to FAK inhibitors remains incomplete. Here, we show that FAK, β5 integrin, and OPN comprise a signaling axis promoting serous ovarian carcinoma tumor growth.

Material and Methods

Antibodies and reagents

PND-1186 (21) (renamed VS-4718 by Verastem Inc.)was from Poniard Inc. and PF-271 was synthesized as described (17). Compounds were dissolved in dimethylsulfoxide (DMSO). Supplemental Table 1 contains antibody, plasmid, and probe sets used in this study. Additional materials and methods, including details of cell cycle, apoptosis and real-time quantitative PCR analyses are described in Supplementary Materials and Methods.

Cells

Supplemental Table 2 lists source, culture conditions, and selective DNA sequencing information for the cells used. Human ovarian cancer cell lines IGROV1, SKOV3 and

SKVO3ip were from J. Chien in 2008 (Mayo Clinic). OVCAR3, OVCAR8 and OVCAR10 cells were from D. Connolly in 2011 (cells generated at Fox Chase) and HEY cells were from S. Howell in 2011 (UCSD). BT474 cells were from ATCC (2008) and maintained in low passages (less than 3 months). For other cells, no authentication was performed by the authors. ID8-IP, IGROV1-IP and SKOV3-IP cells were generated by intraperitoneal injection into nude mice in 2012 as described (12, 22). IGROV1, IGROV1-IP, SKOV3, SKVO3-IP and HEY cells were cultured in Dulbecco's modified Eagle's medium (DMEM); OVCAR3, OVCAR8, OVCAR10, and BT474 cells were culture in RPMI. All cell media was supplemented with 10% fetal bovine serum, 0.1 nM non-essential amino acids, 2 mM glutamine, 100 U/ml penicillin, and 100 μg/ml streptomycin. Cell lines were propagated adherently on plastic and replated on low-binding poly 2-hydroxyethyl methacrylate (poly-HEMA, Corning) coated plates for experimental anchorage-independent analyses.

DNA and retroviral constructs

Short-hairpin (shRNA) targeting human FAK and a scrambled (Scr) control in pLentiLox 3.7-Puro were created as described (23). Lentiviral transduced cells were selected by growth in puromycin: clones were isolated by single cell sorting, and characterized by anti-FAK immunoblotting. Three clones were pooled, expanded, and stored frozen as Scr- or FAK shRNA-expressing HEY cells. Green fluorescent protein (GFP) tagged FAK wildtype (WT) and FAK kinase-dead (KD) from the murine cDNA were cloned into the lentiviral vector pCDH1-MCS1-EF1-Puro (System Biosciences), selected for growth in puromycin, sorted via flow cytometry for GFP expression, and used as a pooled population. HEY cells were transduced with lentiviral shRNAs targeting human β5 integrin or Scr shRNA (Mission, Sigma). HEY and OVCAR8 cells were stably transduced with a myristylated and membrane-targeted form of Akt (Addgene) via retrovirus produced by 293 cell transfection (23).

Cell growth

Cells were plated under adherent (0.5×10^4 cells, tissue culture-treated) and non-adherent conditions (25×10^4 cells, poly-HEMA-coated) in 6-well plates in 2 ml growth media. After 72 h, all cells were collected by limited trypsin–EDTA treatment, a single cell suspension was prepared, and the viable (trypan blue negative) total cell number determined by ViCell XR counting (Beckman). For soft agar assays, 0.2×10^4 cells per well were plated in 0.3% agar in 0.2 ml growth media as described (12). After 7 days, colonies were stained with crystal violet, imaged in phase contrast, and enumerated. All experimental points were performed in triplicate and repeated at least 2 times.

Flow cytometry

For surface integrin expression, cells were trypsinized and incubated with primary antibodies to integrins (10^6 cells / μg antibody) for 20 min on ice and washed in cold PBS. Allophycocyanin (APC)-conjugated goat anti-mouse IgG was used as secondary antibody, and flow cytometry analyses (FACS Calibur) performed using FlowJo software. Mouse IgG was the negative control. For cell cycle analyses, cells were collected as a single cell suspension by limited trypsin treatment and fixed in 70% ethanol. Cells were incubated in 100 μl of PBS containing DNAse-free RNAse (100 μg/ml, Qiagen) and after 45 min,

propidium iodide (PI) (5 μg/ml) was added prior to flow cytometry. For cell apoptosis analyses, cells were stained using APC-conjugated annexin V and 7-amino-actinomycin (7-AAD) (BD Pharmingen), and analyzed within 1 h by flow cytometry.

Protein extracts and immunoblotting

Cell lysis buffer (1% Triton X100, 1% sodium deoxycholic acid, 0.1% SDS, 50 mM Hepes pH 7.4, 150 mM NaCl, 10% glycerol, 1.5 mM MgCl2, 1 mM EGTA, 10 mM sodium pyrophosphate, 100 mM NaF, 1 mM sodium orthovanadate, 10 μg/ml leupeptin, 10 μg/ml aprotinin) was used to extract proteins from cultured cells and tumors as described (12). For conditioned media analyses, cells were cultured in serum-free OptiMEM (Life Technologies) for 24 h, media collected, filtered (0.45 μm), and concentrated using centrifugal filtration (Millipore).

Immunohistochemistry

Paraffin-embedded normal ovarian and ovarian tumor tissue arrays were deparaffinized, rehydrated, processed for antigen retrieval, and peroxidase quenched as described (12). OV811, OV807, OV1502 and OV8010 (US Biomax) slides were used for β5 staining and OV811 used for FAK, pY397 FAK, and OPN. Tissues were blocked (PBS with 5% normal goat serum, 0.5% BSA, and 0.1 % Triton X-100) for 45 min at room temperature (RT) and incubated with anti-pY397 FAK (1:100), anti-FAK (1:100), anti-β5 integrin (1:50), anti-OPN (1:500) in blocking buffer overnight. Biotinylated goat-anti-[rabbit/mouse] IgG or rabbit-anti-goat IgG (1:300), Vectastain ABC Elite, and diaminobenzidine were used to visualize antibody binding. Slides were counter-stained with hematoxylin. Images were captured using an upright microscope (Olympus BX43) with color camera (Olympus SC100). Staining intensity scoring was blinded.

Frozen tumors were thin sectioned (7 μm) using a cryostat (Leica), mounted onto glass slides, fixed with acetone, permeabilized (PBS with 0.1% Triton) for 1 min, and blocked (PBS with 8% goat serum) for 2 h at RT. Sections were incubated in anti-αvβ5 integrin (1:200) in PBS with 2% goat serum overnight, washed, and incubated with goat-anti rabbit Alexa Fluor-647 with Hoechst 33342 to visualize nuclei. Images were acquired using a spinning disc confocal microscope (IX81; Olympus), OrcaER CCD camera (Hamamatsu), pseudo-colored, and merged using Adobe Photoshop.

3D spheroid imaging

Tumor spheroid staining was performed as described (24), with some modifications. Spheroids were fixed and permeabilized for 3 h at 4°C in PBS containing 4% PFA and 1% Triton X-100 with gentle rocking then blocked in PBST (0.1% Triton X-100 in PBS) containing 3% BSA and 8% goat serum overnight at 4°C. Primary anti-pY397FAK (1:100) and anti-OPN (1:500) in PBST were incubated at 4°C for 24 h followed by Alexa Fluor-conjugated secondary antibodies and Hoechst 33342 for 90 min at RT. Spheroids were mounted onto glass slides in 15 μL of PBS with 30 μl of Vectashield and images acquired using a Nikon Eclipse C1 confocal microscope (EZ-C1 3.50 imaging software).

Mouse tumor studies

Eight-week-old female nude (nu/nu) mice (UCSD breeding colony) were housed in pathogen-free conditions. Tumor cells were washed in PBS, injected (2×10^6 cells in 100 μl of PBS) subcutaneously into right and left flanks of nude mice, and tumor volume (length × width^2/2) determined by Vernier caliper measurements over 24 d. Orthotopic tumor growth was initiated by surgical implantation (0.4×10^6 cells in 7 μl of growth factor-depleted Matrigel) within the bursal region surrounding one ovary as described (12). Primary tumor weight was determined following euthanasia upon dissection. Fluorescent images of the intra-abdominal cavity and internal organs were acquired using an OV100 Small Animal Imaging System (Olympus). Blood was collected by heart puncture following euthanasia, samples were centrifuged, and serum was stored at −80°C. The UCSD Institutional Animal Care and Use Committee approved all mouse procedures.

Database analyses

The Kaplan-Meier Plotter (25) was used to query gene expression and survival data from Gene Expression Omnibus and The Cancer Genome Atlas (Affymetrix HG-U133A, HG-U133A 2.0, HG-U133 Plus 2.0 and U95Av2 microarrays). Probes used are listed in Supplemental Table 1. Query parameters were: overall survival, split patients by median, auto-select best cut-off, and follow up threshold of 10 years. Restriction analyses were stage (all), histology (serous), grade (all), optimal debulk (all) and chemotherapy treatments (all). 1038 patient samples were analyzed and Hazard ratio (HR) and logrank P significance were calculated via website interface.

Statistics

Differences between groups were determined using one-way ANOVA with Tukey post hoc analyses (Prism). Differences between pairs of data were determined using an unpaired two-tailed student's t test (Prism). Differences between β5 integrin in normal ovary, stage I and Stages II–IV was determined using the Kruskal-Wallis test. *P*-values of <0.05 were considered significant.

Results

OPN, β5 integrin, and FAK levels correlate with serous ovarian cancer patient survival

Whereas integrins αv and β1 can promote ovarian carcinoma growth, elevated β3 integrin expression may inhibit tumor progression (26, 27). Although increased β5 integrin levels are part of an unfavorable ovarian cancer gene signature (28), limited immunohistochemical analyses detected αvβ5 reactivity only in ovarian tumors of low malignant potential (29). Therefore, connections between αvβ5 integrin and ovarian tumor progression remain unclear. We evaluated the importance of β5, αv, β3, and β1 integrin mRNA levels in a large annotated database of ovarian cancer patient samples (Fig. 1). Kaplan-Meier analyses showed that elevated β5, αv, and β1 integrin levels are significantly associated with decreased patient survival (Fig. 1A). In contrast, β3 integrin levels were not associated with patient survival differences (Fig. 1A). Expression of matrix ligands for αvβ5 integrins such

as OPN and a downstream target of αvβ5 signaling such as FAK, were also significantly associated with decreased patient survival (Fig. 1A).

Increased β5 integrin staining in stage II–IV serous ovarian tumors

As determined by tumor staining, increased FAK, pY397 FAK, and OPN levels correlate with a poor ovarian cancer patient prognosis (6, 30, 31). Staining of tumor tissue array serial sections with antibodies to OPN, FAK, FAK pY397, and β5 integrin revealed parallel increases as a function of tumor stage (Fig. 1B and Supplemental Fig. S1A). Specificity of FAK pY397 staining was confirmed by analyses of ID8-IP ovarian tumors from mice treated with vehicle or PF-271 FAK inhibitor (Supplemental Fig. S1B). Additional tumor tissue array staining analyses revealed no difference between β5 integrin levels in normal ovary tissue and Stage I serous tumors (Fig. 1C). However, analyses of advanced Stage II–IV tumors that present foci of dissemination showed significantly increased β5 integrin staining compared to Stage I tumors, that are confined to the ovary (Fig. 1C, $p<0.05$). Together with the mRNA array analyses, these results support the hypothesis that OPN, αvβ5 integrin, and FAK activity may function as a signaling axis promoting ovarian tumor progression. Moreover, β5 integrin expression may serve as a biomarker for serous ovarian carcinoma cells that possess active FAK.

Identification of FAK inhibitor sensitive and resistant ovarian cancer cells

Analyses of seven ovarian carcinoma cell lines in anchorage-independent growth assays identified sensitive (HEY, OVCAR8) and resistant (SKOV3-IP, OVCAR10) cells to 0.1 μM FAK inhibitor (VS-4718) addition (Fig. 2A). SKOV3-IP and OVCAR10 cells remained resistant with up to 1.0 μM VS-4718 for 72 h whereas OVCAR3, ID8-IP, and IGROV1-IP cells exhibited an intermediate growth inhibitory response. Flow cytometry analyses were performed to determine whether VS-4718 (1 μM, 72 h) triggered cell death (7-AAD staining and annexin V binding) and/or alterations in cell cycle progression in sensitive (HEY, OVCAR8) or resistant (SKOV3-IP, OVCAR10) cells. Early (annexin V positive) and late (annexin V and 7-AAD positive cells)OVCAR8 apoptotic cells were detected as well OVCAR8 cells with G0/G1 block and decreased S phase cell cycle percentage upon VS-4718 treatment (Supplemental Fig. S2). HEY cells did not exhibit changes in apoptosis, but VS-4718 blocked HEY cell cycle progression (Supplemental Fig. S2). Treatment of OVCAR10 or SKOV3-IP resistant cells with 1 μM VS-4718 did not alter cell cycle progression or promote cell death (Supplemental Fig. S2). Thus, in sensitive cells, FAK inhibitor treatment promotes G0/G1 cell cycle arrest followed by cell death.

Previous studies implicated the PI3K/Akt kinase pathway as a downstream target of FAK in ovarian tumor cells (31, 32). Akt activation is common in high-grade, late-stage serous ovarian tumors (33). To gain insights into molecular targets altered by FAK inhibitor treatment, immunoblotting analyses were performed on lysates of sensitive (HEY, OVCAR8) and resistant (OVCAR10, SKOV3-IP) cells grown in suspension for 72 h in the presence or absence of 1 μM VS-4718 (Fig. 2B). VS-4718 prevented FAK Y397 phosphorylation in SKOV3-IP, HEY, and OVCAR8 cells whereas FAK Y397 phosphorylation was already low in OVCAR10 cells. Resistant OVCAR10 and SKOV3-IP cells had high Akt S473 phosphorylation and no changes in β5 integrin levels upon VS-4718

addition (Fig. 2B). In contrast, Akt S473 phosphorylation was not detected and β5 integrin levels were decreased in VS-4718-treated sensitive HEY and OVCAR8 cells, compared to controls. These results suggest that FAK inhibitor resistant cells may contain genetic alterations promoting Akt S473 phosphorylation and that FAK activation may be part of a signaling loop controlling β5 integrin levels in sensitive cells.

FAK activity regulates β5 integrin expression and anchorage-independent cell growth

Intraperitoneal (IP) growth of murine ID8 ovarian carcinoma cells followed by *in vitro* culture resulted in the isolation of aggressive cells, named ID8-IP (12). Compared to parental ID8 cells, FAK Y397 phosphorylation (pY397 FAK), β5 integrin, and OPN levels are elevated in ID8-IP cells under anchorage-independent conditions (Fig. 3A). In both ID8-IP and HEY cells, 1 μM VS-4718 treatment selectively lowers pY397 FAK, β5 integrin, and OPN levels (Figs. 3B–D). To confirm that this was due to FAK inactivation, HEY cells were transduced with scrambled (Scr) or FAK shRNA to knockdown FAK expression ~90% (Fig. 3E). GFP-tagged FAK-WT or -KD (kinase dead) were stably re-expressed in HEY FAK shRNA cells at equivalent levels (Figs. 3E and F). GFP-FAK-WT cells exhibited elevated pY397 FAK compared to GFP-FAK-KD cells (Fig. 3F).

To determine if loss of FAK expression or activity altered HEY cell growth, analyses were performed under adherent, suspended, and soft agar conditions (Figs. 3G–I). No growth differences were noted when cells were grown on plastic (Fig. 3G), but FAK knockdown reduced growth in suspension and soft agar (Figs. 3H and I). This was rescued by GFP-FAK-WT but not GFP-FAK-KD re-expression. Correspondingly, FAK knockdown reduced HEY growth as subcutaneous tumors and this was rescued by GFP-FAK-WT but not GFP-FAK-KD re-expression (Figs. 4A and B). GFP-FAK WT also promoted orthotopic HEY tumor growth and spontaneous peritoneal metastasis that was significantly reduced in HEY cells expressing GFP-FAK-KD (Figs. 4C and D). These results show that FAK activity is important for anchorage-independent and ovarian tumor growth.

Analyses of HEY tumors showed reduced pY397 FAK, OPN and αvβ5 integrin levels in GFP-FAK-KD compared to GFP-FAK-WT tumors (Figs. 4E and F). Immunoblotting ID8-IP tumor lysates showed that oral FAK inhibitor administration reduced pY397 FAK, OPN, and β5 integrin levels compared to vehicle control-treated mice (Supplemental Fig. S3). Interestingly, quantitative PCR revealed no changes in β5 integrin mRNA levels upon genetic or pharmacological FAK inhibition in HEY cells (Supplemental Fig. S4). Together, these results show that the inhibition of FAK activity in HEY cells decreases tumor growth with a corresponding reduction in β5 integrin protein levels that occurs independently of changes in β5 integrin mRNA expression.

β5 integrin promotes HEY ovarian tumor growth

To determine whether FAK and β5 integrin comprise a signaling axis promoting ovarian tumor growth, two independent lentiviral shRNAs were used to stably knockdown HEY β5 integrin expression (Fig. 5A). Flow cytometry analyses showed that αvβ5 integrin was reduced ~10-fold on the surface of HEY cells (Fig. 5B). HEY β5 integrin knockdown did not result in compensatory increases in αvβ3 or β1 integrin surface expression

(Supplemental Fig. S5). β5 knockdown minimally impacted the growth of HEY cells in adherent conditions compared to the scrambled control (Fig. 5C). In contrast, β5 knockdown significantly reduced HEY growth in soft agar (Fig. 5D). This was associated with decreased FAK Y397 phosphorylation and OPN expression as determined by immunofluorescent staining of spheroids (Fig. 5E). When injected orthotopically into the ovarian bursa space, HEY β5 integrin knockdown cells resulted in decreased tumor size after 21 days and reduced serum levels of cleaved (25 kDa) human OPN (Figs. 5F and G). Together, these results show that the FAK-β5 integrin signaling axis promotes HEY tumor growth and that OPN may serve as a secreted ligand in this pathway.

Partial phenotypic rescue by activated Akt expression

FAK inhibitor resistant SKOV3-IP and OVCAR10 cells exhibited elevated Akt S473 phosphorylation, an indirect marker of Akt activation in anchorage-independent conditions (Fig. 2B). One possible explanation is that SKOV3-IP cells contain activating mutations in *PIK3CA* (Supplemental Table 2) and this may bypass effects of upstream FAK inhibition. Moreover, studies have shown that inhibition of mTOR (mammalian target of rapamycin), a downstream target of Akt, prevents SKOV3 and OVCAR10 cell growth (34). To determine if Akt activation is sufficient to bypass FAK inhibition, membrane-targeted myristylated Akt (Akt*) was stably expressed in sensitive HEY and OVCAR8 cells (Fig. 6). Immunoblotting of lysates showed that Akt*remained highly phosphorylated at S473 and T308 in the presence of 1 μM VS-4718treatment of cells for 72 h in suspension (Fig. 6A). Although Akt* remained active, FAK Y397 phosphorylation was equally reduced by VS-4718 addition in control vector (CTRL) and Akt*-expressing HEY and OVCAR8 cells (Fig. 6A). These results are consistent with Akt being downstream of FAK.

To test the effects of Akt* on suspended cell growth, CTRL and Akt*-expressing HEY and OVCAR8 cells were grown in suspension in the presence or absence of 1 μM VS-4718treatment for 72 h (Fig. 6B). CTRL HEY and OVCAR8 cells remained highly sensitive to FAK inhibitor addition (70% growth inhibition) and surprisingly, Akt*-expressing cells showed ~50% growth inhibition to VS-4718. Although this was significantly higher than CTRL cells, Akt* did not completely suppress HEY and OVCAR8 sensitivity to VS-4718 growth inhibition (Fig. 6B). When resistant OVCAR10 cells were treated with VS-4718 in combination with wortmannin (a PI3-kinase inhibitor), anchorage-independent growth and Akt S373 phosphorylation were decreased (Fig. 6C). Finally, when analyzing β5 integrin surface expression, there was a significant reduction in CTRL HEY cells upon VS-4718 addition and this reduction was not observed in HEY Akt* cells (Fig. 6D). These results support the conclusion that FAK to Akt signaling is important for maintenance of β5 integrin surface expression. However, ovarian tumor growth resistance to FAK inhibitor treatment likely involves multiple pathways in addition to Akt activation.

Discussion

The high mortality rate in ovarian cancer is partially due to its unusual mechanism of dissemination. Cells are shed from the primary tumor into the peritoneal cavity where tumor growth occurs in an anchorage-independent manner as clumps of aggregated cells termed

spheroids (2). Under these conditions, interactions between integrins and matrix proteins promote cell survival and proliferation. We find that pharmacological and genetic inhibition of FAK decreases ovarian carcinoma β5 integrin and OPN levels in tumors. This role for FAK activity is distinct from the canonical linkage of matrix-integrin binding leading to FAK activation (32). FAK inhibition or β5 knockdown reduced ovarian tumor cell growth under anchorage-independent conditions with corresponding decreases in orthotopic tumor growth. High OPN, β5 integrin and FAK mRNA levels are associated with decreased survival of serous ovarian cancer patients and immunohistochemical analyses confirmed that protein levels correlate with increasing serous ovarian tumor stage. Our results support a model whereby FAK inhibition disrupts autocrine-paracrine signaling regulating β5 integrin and OPN levels in ovarian carcinoma cells.β5 integrin expression may serve as a biomarker for serous ovarian carcinoma cells that possess active FAK signaling. Moreover, reduction of β5 integrin levels may serve as an indicator of FAK inhibitor effectiveness in ovarian cancer.

Notably, genetic and pharmacological FAK inhibition prevented anchorage-independent but not adherent ovarian cancer cell growth. Moreover, we identified cells as either sensitive (HEY, OVCAR8) or resistant (SKOV3-IP, OVCAR10) to VS-4718 treatment. Despite the fact that several drugs have low efficacy on tumor cells cultured as spheroids (35, 36), nanomolar concentrations of VS-4718 prevented sensitive ovarian cancer cell growth as spheroids by triggering cell cycle blockage and apoptosis. As FAK inhibitors are being tested in clinical trials, it is important to identify molecular drivers of potential resistance as a means to select patients that may preferentially benefit from FAK inhibitor treatment.

Analysis of mutation frequency, copy number, or gene expression changes revealed that ~45% of serous ovarian cancer contain some type of alteration that would activate *PI3K* and *RAS* signaling pathways (37). Interestingly, studies have found that pharmacologic FAK inhibition (PF-271, 40 mg/kg) decreased tumor volume in a *KRAS* G12D mouse model of non-small cell lung carcinoma and human lung tumor cell xenografts (38). Additionally, VS-4718 (PND-1186) FAK inhibition was effective in preventing MDA-MB-231 (*KRAS* G12V and *BRAF* V600E) breast carcinoma orthotopic tumor growth and metastasis (18). Sequencing of the HEY-A8 ovarian tumor sub-clone reveals *KRAS* G12D and *BRAF* G464E activating mutations (Supplemental Table 2) (39), and HEY-A8 cells are responsive to pharmacological FAK inhibition (Verastem, VS-6063) (31). Since HEY cells are sensitive to VS-4718 FAK inhibition, these studies support the notion that *KRAS*- and *BRAF* oncogenic mutations do not confer a FAK inhibitor resistant phenotype.

Further, it is known that PI3K and Akt activation can be downstream targets of FAK signaling in ovarian cancer (31, 32). Sequencing of SKOV3 and IGROV-1 ovarian tumor cells has revealed activating mutations in *PIK3CA* (Supplemental Table 2) (39). Although combined PI3K and FAK inhibition had additive effects in preventing OVCAR10 anchorage-independent growth, expression of activated Akt was not sufficient to generate a FAK inhibitor resistant phenotype in HEY or OVCAR8 cells. Together, these results support the notion that FAK signaling impacts a growth promoting pathway distinct from that activated by oncogenic mutations in *KRAS, BRAF, and PIK3CA*.

Supplementary Material

Refer to Web version on PubMed Central for supplementary material.

Acknowledgments

We thank David Tarin for providing guidance and expertise in tumor pathology.

Grant support

This work was supported by National Institutes of Health grant CA102310 and a grant from “Nine Girls Ask?” to D. Schlaepfer. I. Tancioni was supported by a grant from Susan G. Komen for the Cure (KG111237). F. Sulzmaier was supported by National Institutes of Health training grant (T32-CA121938). C. Lawson was supported in part by an Ovarian Cancer Research Fund fellowship (258835). C. Jean was supported by an American Heart Association fellowship (12POST11760014). N.L.G. Miller was supported by a National Research Service Award (1F32CA159558). N. Shah and K. Ward are fellows of the UCSD Reproductive Medicine Gynecologic Oncology program.

References

1. Siegel R, Ma J, Zou Z, Jemal A. Cancer statistics, 2014. CA: a cancer journal for clinicians. 2014; 64:9–29. [PubMed: 24399786]
2. Shield K, Ackland ML, Ahmed N, Rice GE. Multicellular spheroids in ovarian cancer metastases: Biology and pathology. Gynecol Oncol. 2009; 113:143–8. [PubMed: 19135710]
3. Hanahan D, Weinberg RA. Hallmarks of cancer: the next generation. Cell. 2011; 144:646–74. [PubMed: 21376230]
4. Kipps E, Tan DS, Kaye SB. Meeting the challenge of ascites in ovarian cancer: new avenues for therapy and research. Nat Rev Cancer. 2013; 13:273–82. [PubMed: 23426401]
5. Carduner L, Agniel R, Kellouche S, Picot CR, Blanc-Fournier C, Leroy-Dudal J, et al. Ovarian cancer ascites-derived vitronectin and fibronectin: combined purification, molecular features and effects on cell response. Biochim Biophys Acta. 2013; 1830:4885–97. [PubMed: 23811340]
6. Kim JH, Skates SJ, Uede T, Wong KK, Schorge JO, Feltmate CM, et al. Osteopontin as a potential diagnostic biomarker for ovarian cancer. Jama-J Am Med Assoc. 2002; 287:1671–9.
7. Visintin I, Feng Z, Longton G, Ward DC, Alvero AB, Lai Y, et al. Diagnostic markers for early detection of ovarian cancer. Clin Cancer Res. 2008; 14:1065–72. [PubMed: 18258665]
8. Casey RC, Burleson KM, Skubitz KM, Pambuccian SE, Oegema TR Jr, Ruff LE, et al. Beta 1-integrins regulate the formation and adhesion of ovarian carcinoma multicellular spheroids. Am J Pathol. 2001; 159:2071–80. [PubMed: 11733357]
9. Iwanicki MP, Davidowitz RA, Ng MR, Besser A, Muranen T, Merritt M, et al. Ovarian cancer spheroids use myosin-generated force to clear the mesothelium. Cancer discovery. 2011; 1:144–57. [PubMed: 22303516]
10. Mitra AK, Sawada K, Tiwari P, Mui K, Gwin K, Lengyel E. Ligand-independent activation of c-Met by fibronectin and alpha(5)beta(1)-integrin regulates ovarian cancer invasion and metastasis. Oncogene. 2011; 30:1566–76. [PubMed: 21119598]
11. Bell-McGuinn KM, Matthews CM, Ho SN, Barve M, Gilbert L, Penson RT, et al. A phase II, single-arm study of the anti-alpha5beta1 integrin antibody volociximab as monotherapy in patients with platinum-resistant advanced epithelial ovarian or primary peritoneal cancer. Gynecol Oncol. 2011; 121:273–9. [PubMed: 21276608]
12. Ward KK, Tancioni I, Lawson C, Miller NL, Jean C, Chen XL, et al. Inhibition of focal adhesion kinase (FAK) activity prevents anchorage-independent ovarian carcinoma cell growth and tumor progression. Clin Exp Metastasis. 2013; 30:579–94. [PubMed: 23275034]
13. Desgrosellier JS, Cheresh DA. Integrins in cancer: biological implications and therapeutic opportunities. Nat Rev Cancer. 2010; 10:9–22. [PubMed: 20029421]

14. Slack-Davis JK, Martin KH, Tilghman RW, Iwanicki M, Ung EJ, Autry C, et al. Cellular characterization of a novel focal adhesion kinase inhibitor. J Biol Chem. 2007; 282:14845–52. [PubMed: 17395594]
15. Lim ST, Chen XL, Tomar A, Miller NL, Yoo J, Schlaepfer DD. Knock-in mutation reveals an essential role for focal adhesion kinase activity in blood vessel morphogenesis and cell motility-polarity but not cell proliferation. J Biol Chem. 2010; 285:21526–36. [PubMed: 20442405]
16. Halder J, Lin YG, Merritt WM, Spannuth WA, Nick AM, Honda T, et al. Therapeutic efficacy of a novel focal adhesion kinase inhibitor TAE226 in ovarian carcinoma. Cancer Res. 2007; 67:10976–83. [PubMed: 18006843]
17. Roberts WG, Ung E, Whalen P, Cooper B, Hulford C, Autry C, et al. Antitumor activity and pharmacology of a selective focal adhesion kinase inhibitor, PF-562, 271. Cancer Res. 2008; 68:1935–44. [PubMed: 18339875]
18. Walsh C, Tanjoni I, Uryu S, Tomar A, Nam JO, Luo H, et al. Oral delivery of PND-1186 FAK inhibitor decreases tumor growth and spontaneous breast to lung metastasis in pre-clinical models. Cancer Biol Ther. 2010; 9:778–90. [PubMed: 20234193]
19. Tanjoni I, Walsh C, Uryu S, Tomar A, Nam JO, Mielgo A, et al. PND-1186 FAK inhibitor selectively promotes tumor cell apoptosis in three-dimensional environments. Cancer Biol Ther. 2010; 9:764–77. [PubMed: 20234191]
20. Infante JR, Camidge DR, Mileshkin LR, Chen EX, Hicks RJ, Rischin D, et al. Safety, pharmacokinetic, and pharmacodynamic phase I dose-escalation trial of PF-00562271, an inhibitor of focal adhesion kinase, in advanced solid tumors. J Clin Oncol. 2012; 30:1527–33. [PubMed: 22454420]
21. Heinrich T, Seenisamy J, Emmanuvel L, Kulkarni SS, Bomke J, Rohdich F, et al. Fragment-based discovery of new highly substituted 1H-pyrrolo[2,3-b]- and 3H-imidazolo[4,5-b]-pyridines as focal adhesion kinase inhibitors. J Med Chem. 2013; 56:1160–70. [PubMed: 23294348]
22. Yu D, Wolf JK, Scanlon M, Price JE, Hung MC. Enhanced c-erbB-2/neu expression in human ovarian cancer cells correlates with more severe malignancy that can be suppressed by E1A. Cancer Res. 1993; 53:891–8. [PubMed: 8094034]
23. Lim ST, Chen XL, Lim Y, Hanson DA, Vo TT, Howerton K, et al. Nuclear FAK promotes cell proliferation and survival through FERM-enhanced p53 degradation. Mol Cell. 2008; 29:9–22. [PubMed: 18206965]
24. Weiswald LB, Guinebretiere JM, Richon S, Bellet D, Saubamea B, Dangles-Marie V. In situ protein expression in tumour spheres: development of an immunostaining protocol for confocal microscopy. BMC Cancer. 2010; 10:106. [PubMed: 20307308]
25. Gyorffy B, Lanczky A, Szallasi Z. Implementing an online tool for genome-wide validation of survival-associated biomarkers in ovarian-cancer using microarray data from 1287 patients. Endocrine-related cancer. 2012; 19:197–208. [PubMed: 22277193]
26. Davidson B, Goldberg I, Reich R, Tell L, Dong HP, Trope CG, et al. AlphaV- and beta1-integrin subunits are commonly expressed in malignant effusions from ovarian carcinoma patients. Gynecol Oncol. 2003; 90:248–57. [PubMed: 12893184]
27. Kaur S, Kenny HA, Jagadeeswaran S, Zillhardt MR, Montag AG, Kistner E, et al. {beta}3-integrin expression on tumor cells inhibits tumor progression, reduces metastasis, and is associated with a favorable prognosis in patients with ovarian cancer. Am J Pathol. 2009; 175:2184–96. [PubMed: 19808644]
28. Spentzos D, Levine DA, Ramoni MF, Joseph M, Gu X, Boyd J, et al. Gene expression signature with independent prognostic significance in epithelial ovarian cancer. J Clin Oncol. 2004; 22:4700–10. [PubMed: 15505275]
29. Grisaru-Granovsky S, Salah Z, Maoz M, Pruss D, Beller U, Bar-Shavit R. Differential expression of protease activated receptor 1 (Par1) and pY397FAK in benign and malignant human ovarian tissue samples. International journal of cancer Journal international du cancer. 2005; 113:372–8. [PubMed: 15455382]
30. Sood AK, Coffin JE, Schneider GB, Fletcher MS, DeYoung BR, Gruman LM, et al. Biological significance of focal adhesion kinase in ovarian cancer: role in migration and invasion. Am J Pathol. 2004; 165:1087–95. [PubMed: 15466376]

31. Kang Y, Hu W, Ivan C, Dalton HJ, Miyake T, Pecot CV, et al. Role of Focal Adhesion Kinase in Regulating YB-1-Mediated Paclitaxel Resistance in Ovarian Cancer. J Natl Cancer Inst. 2013; 105:1485–95. [PubMed: 24062525]
32. Lane D, Goncharenko-Khaider N, Rancourt C, Piche A. Ovarian cancer ascites protects from TRAIL-induced cell death through alphavbeta5 integrin-mediated focal adhesion kinase and Akt activation. Oncogene. 2010; 29:3519–31. [PubMed: 20400979]
33. Altomare DA, Wang HQ, Skele KL, De Rienzo A, Klein-Szanto AJ, Godwin AK, et al. AKT and mTOR phosphorylation is frequently detected in ovarian cancer and can be targeted to disrupt ovarian tumor cell growth. Oncogene. 2004; 23:5853–7. [PubMed: 15208673]
34. Mabuchi S, Altomare DA, Connolly DC, Klein-Szanto A, Litwin S, Hoelzle MK, et al. RAD001 (Everolimus) delays tumor onset and progression in a transgenic mouse model of ovarian cancer. Cancer Res. 2007; 67:2408–13. [PubMed: 17363557]
35. Friedrich J, Ebner R, Kunz-Schughart LA. Experimental anti-tumor therapy in 3-D: spheroids–old hat or new challenge? Int J Radiat Biol. 2007; 83:849–71. [PubMed: 18058370]
36. Friedrich J, Seidel C, Ebner R, Kunz-Schughart LA. Spheroid-based drug screen: considerations and practical approach. Nat Protoc. 2009; 4:309–24. [PubMed: 19214182]
37. Cancer Genome Atlas Research N. Integrated genomic analyses of ovarian carcinoma. Nature. 2011; 474:609–15. [PubMed: 21720365]
38. Konstantinidou G, Ramadori G, Torti F, Kangasniemi K, Ramirez RE, Cai Y, et al. RHOA-FAK is a required signaling axis for the maintenance of KRAS-driven lung adenocarcinomas. Cancer discovery. 2013; 3:444–57. [PubMed: 23358651]
39. Domcke S, Sinha R, Levine DA, Sander C, Schultz N. Evaluating cell lines as tumour models by comparison of genomic profiles. Nature communications. 2013; 4:2126.

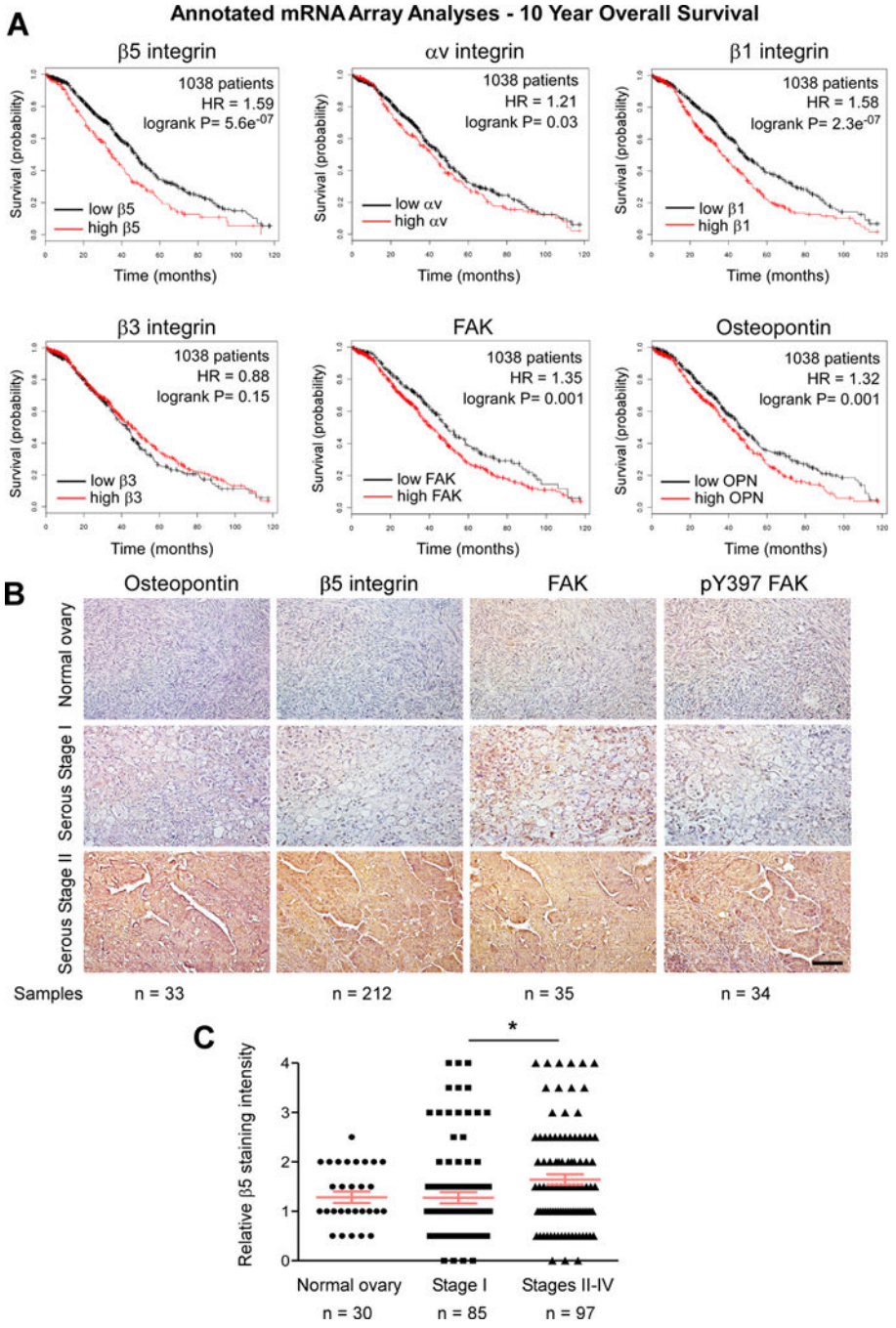

Figure 1.

Association between OPN, β5 integrin, and FAK activation in serous ovarian cancer. A, Kaplan-Meier analyses of integrin β5, αv, β1, β3, FAK, and OPN mRNA levels in 1038 patient samples. High (*red*) versus low (*black*) mRNA expression shows patient overall survival probability over 120 months. Hazard ratio (HR) and logrank P significance values are shown (inset). B, representative immunohistochemical staining of sections obtained from paraffin-embedded normal ovary, serous Stage I, and serous Stage II ovarian tumor tissue arrays using antibodies to pY397 FAK, total FAK, β5 integrin, and OPN. Scale is 100 μm.

C, β5 integrin staining intensity (0–4) in annotated ovarian tissue arrays. Values are means (+/− SEM, * $p < 0.05$, n= sample number).

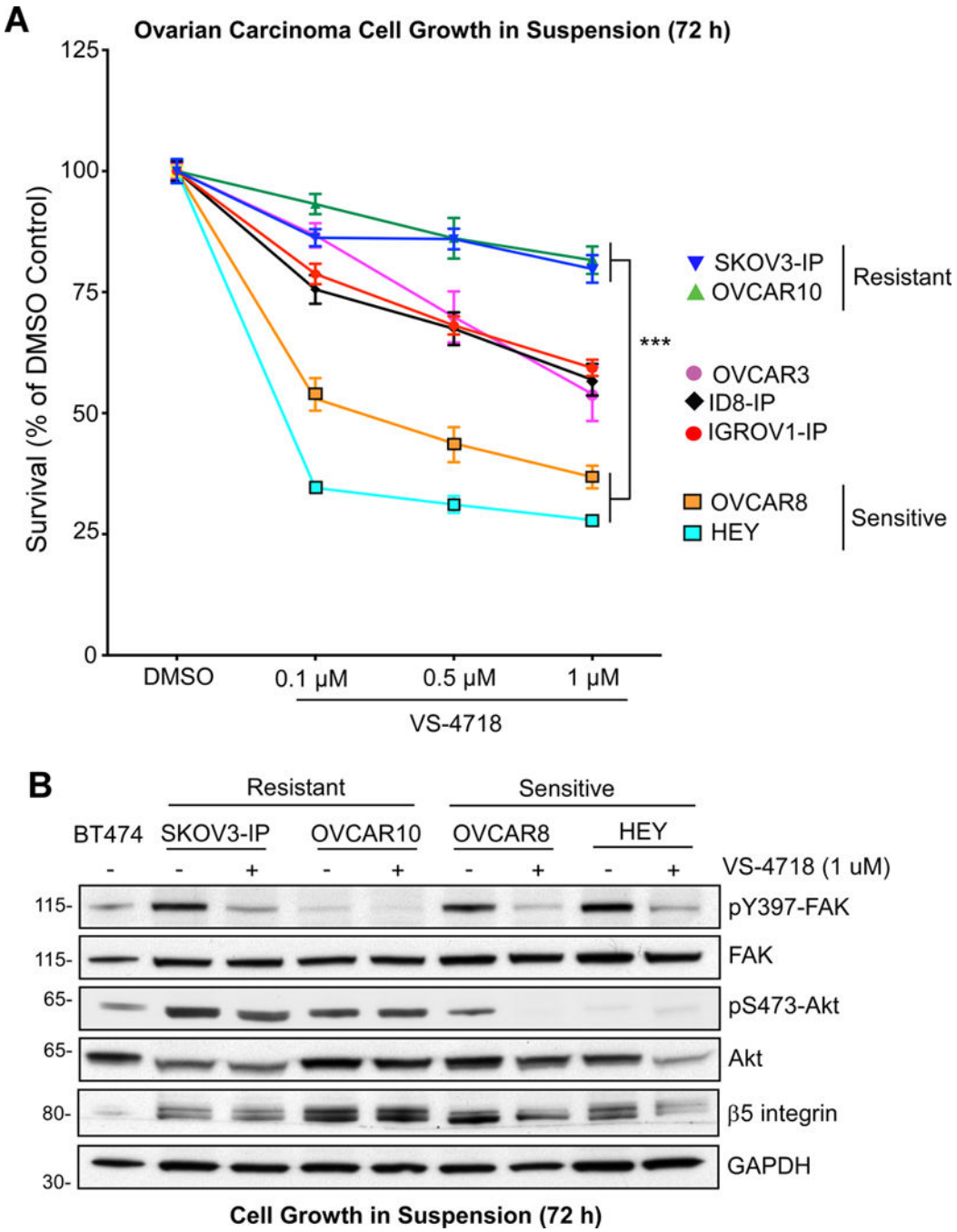

Figure 2.

Identification of FAK inhibitor sensitive and resistant ovarian carcinoma cells. A, the indicated ovarian carcinoma cell lines were evaluated for anchorage-independent growth over 72 h in DMSO (control) or increasing concentrations of VS-4718 (0.1 to 1.0 μM). Values are means (+/− SEM) of triplicate points from three independent experiments (*** $p<0.001$ versus control). B, lysates of the indicated cells cultured in suspension with DMSO or VS-4718 (1 μM) for 72 h were analyzed by immunoblotting for pY397 FAK, pS473

AKT, and β5 integrin levels. Corresponding levels of total FAK, Akt, and GAPDH are shown. BT474 breast carcinoma cells are a positive control for pS473 AKT.

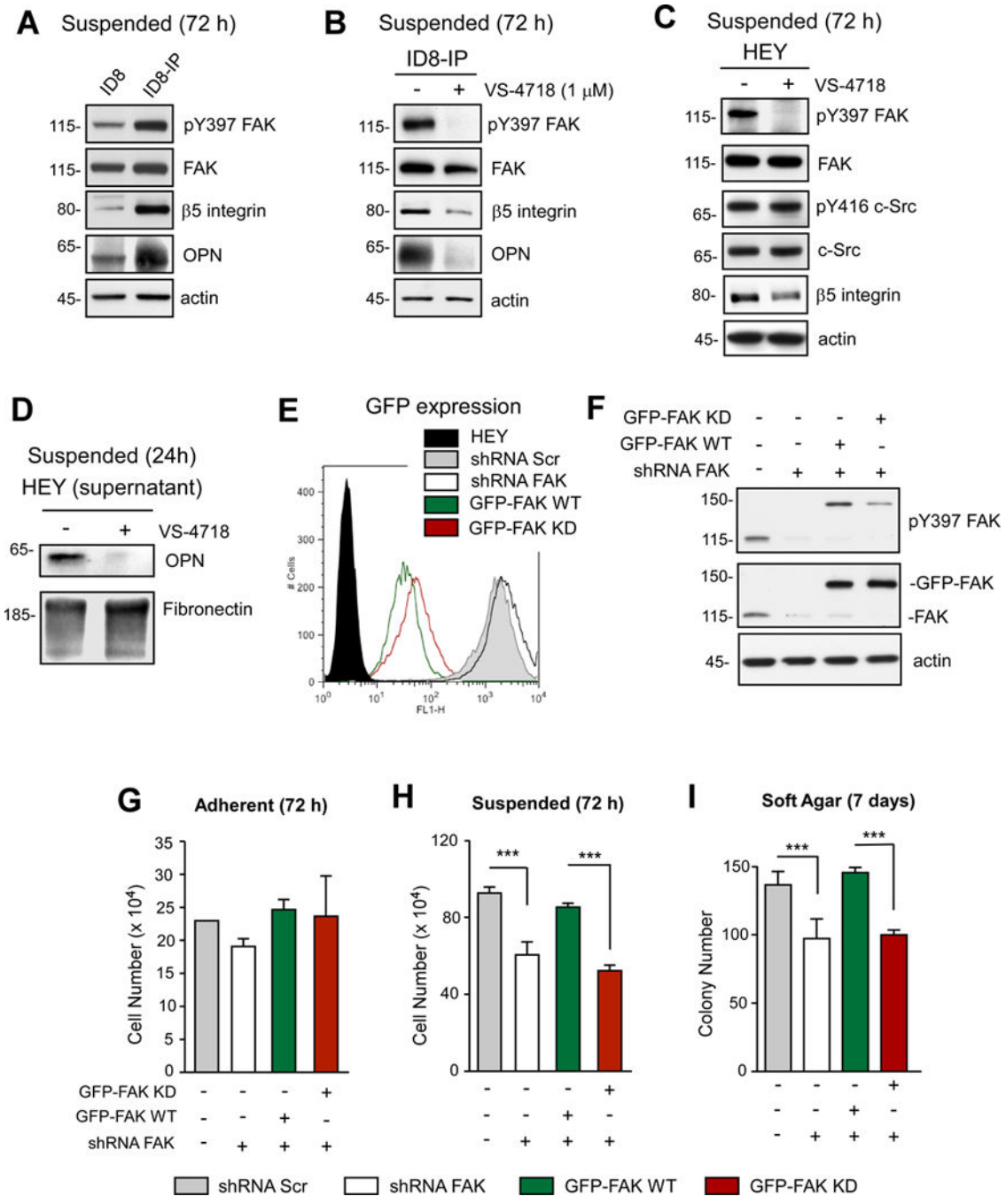

Figure 3.

FAK inhibition reduces β5 integrin and OPN levels in ID8-IP and HEY cells. A, lysates of ID8 and ID8-IP cells grown in suspension for 72 h immunoblotted for pY397 FAK, total FAK, β5 integrin, OPN, and actin. B, lysates of DMSO- or VS-4718-treated ID8-IP cells grown in suspension for 72 h immunoblotted for pY397 FAK, total FAK, β5 integrin, OPN, and actin. C, DMSO- or VS-4718-treated HEY cells in suspension for 72 h were immunoblotted for pY397 FAK, FAK, Src pY416, c-Src, β5 integrin, OPN, and actin. D, conditioned media from anchorage-independent 24 h DMSO- or VS-4718-treated HEY cells

were immunoblotted for OPN and fibronectin. E, stable lentiviral scrambled (Scr, gray) or FAK shRNA (white) knockdown HEY cells were transduced to express GFP, GFP-FAK-WT (green), or GFP-FAK KD (red) and analyzed by flow cytometry. Black histogram, parental HEY background fluorescence. F, HEY cells knocked down and reconstituted with FAK were immunoblotted for exogenous GFP-FAK (~150 kDa) and endogenous FAK (~115 kDa) pY397 FAK and total FAK. Actin is a loading control. G–I, growth of Scr shRNA (gray), FAK shRNA, (white), GFP-FAK WT- (green), and GFP-FAK KD-reconstituted (red) HEY cells in adherent (G), suspended (H), and soft agar (I) growth conditions at 72 hr. Values are means (+/− SD) of triplicate points (***$p<0.001$) from at least two independent experiments.

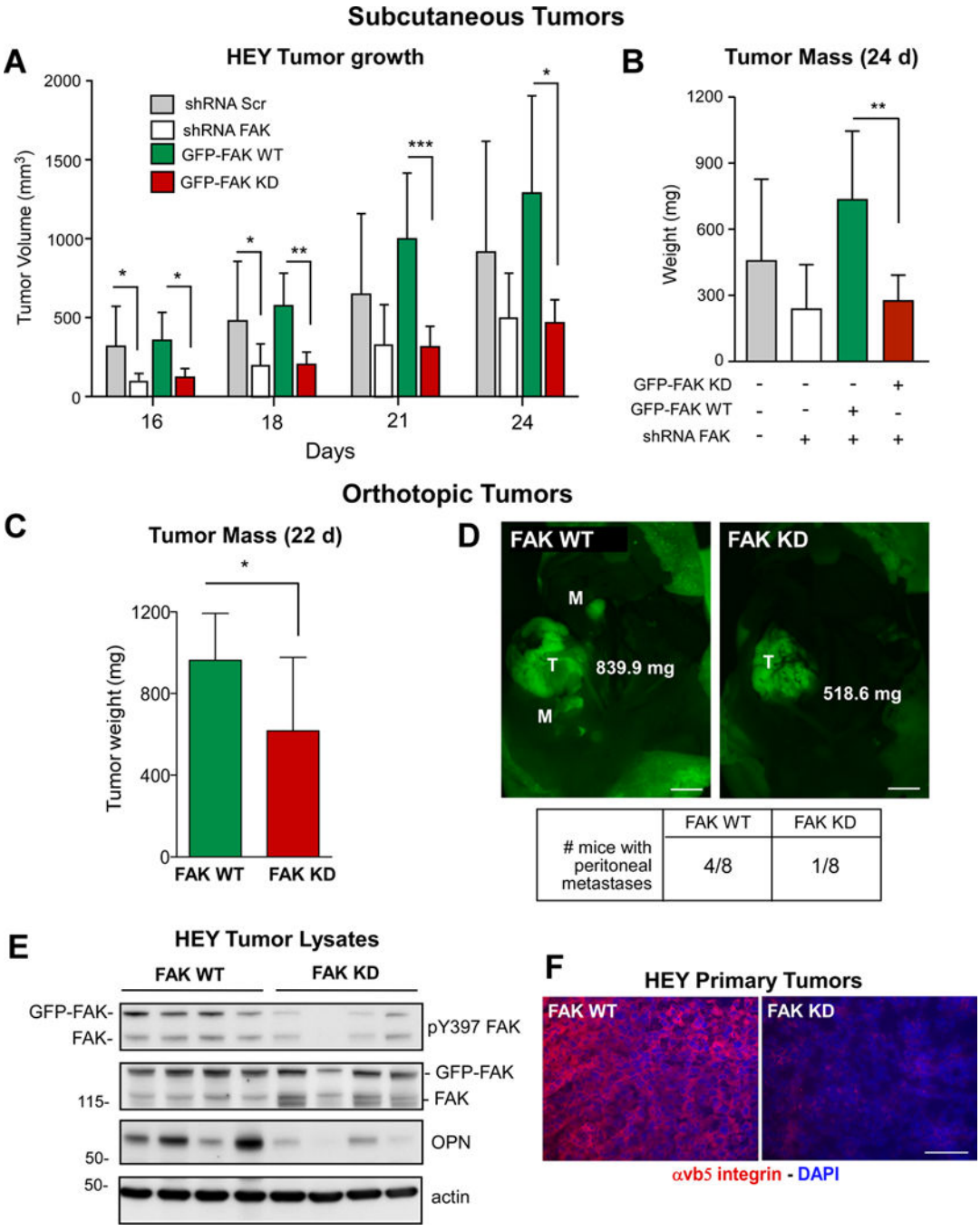

Figure 4.

Genetic FAK inhibition prevents HEY tumor growth associated with decreased OPN and β5 integrin levels. A, mean subcutaneous tumor volume of Scr shRNA (gray, n=6), FAK shRNA (white, n=6), GFP-FAK WT- (green, n=5), and GFP-FAK KD-reconstituted (red, n=6) HEY cells at day 16 to 24 (+/− SD, * p< 0.05, ** p< 0.01; *** p<0.0001). B, final mean subcutaneous tumor mass in panel A (+/− SD, ** p< 0.01). C, Mean GFP-FAK WT (green, n=8), and GFP-FAK KD (red, n=8) HEY orthotopic tumor mass (+/− SD, *p< 0.05). D, representative orthotopic tumors (T) and peritoneal metastasis sites (M) as determined by

GFP fluorescent imaging. Scale is 0.5 cm. E, lysates from four GFP-FAK WT or four GFP-FAK KD HEY orthotopic tumors analyzed by pY397 FAK, total FAK, OPN, and actin immunoblotting. F, fluorescent microscopic images of GFP-FAK WT and GFP-FAK-KD HEY tumor sections stained for αvβ5 integrin (red) and cell nuclei (blue). Scale is 100 μm.

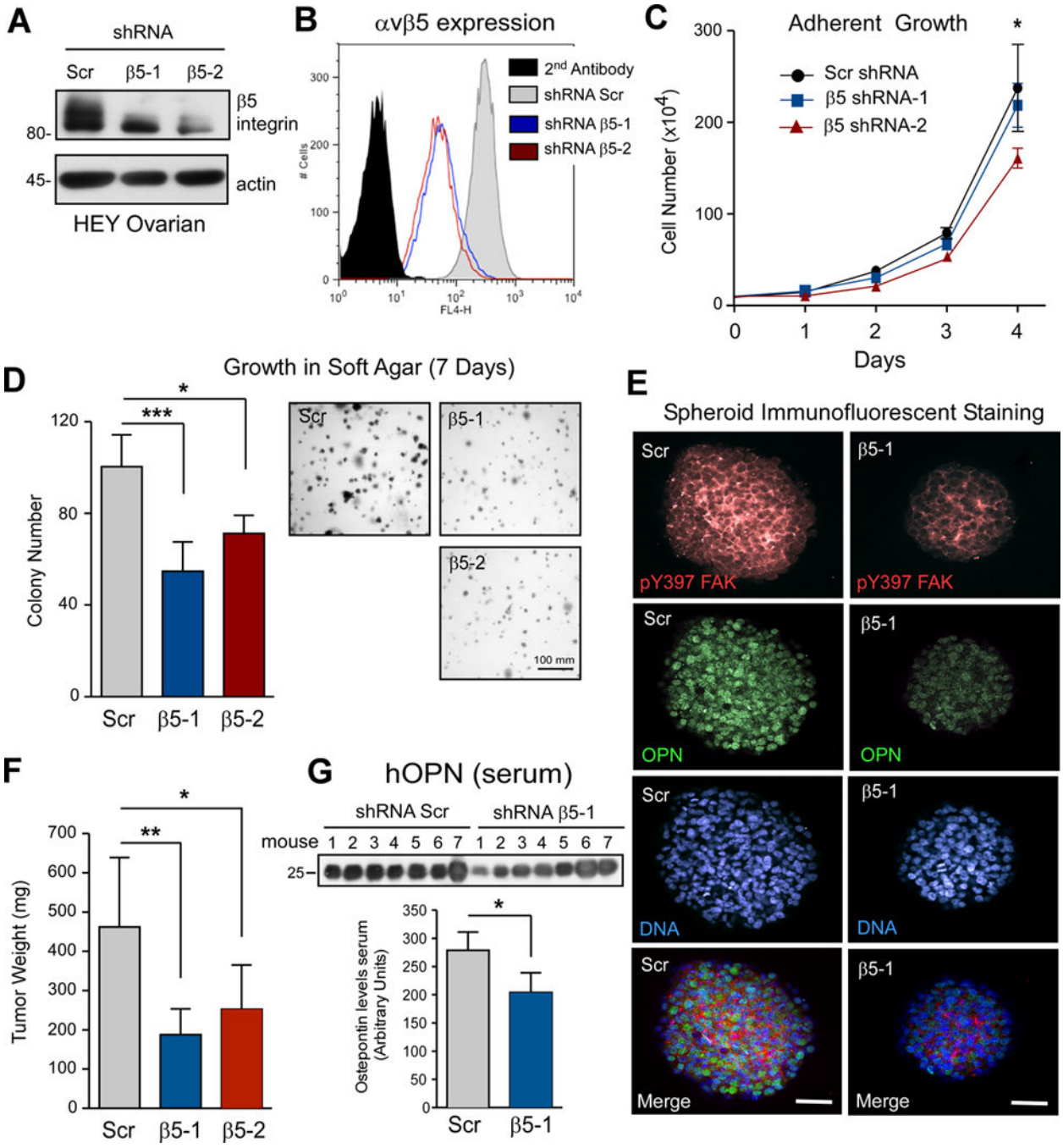

Figure 5.

HEY β5 integrin knockdown impairs soft agar and tumor growth with reduced FAK Y397 phosphorylation in spheroids. A, stable HEY β5 integrin knockdown by lentiviral shRNAs (β5-1 and β5-2) as determined by immunoblotting with actin as a loading control. B, flow cytometry of cell surface αvβ5 levels in Scr, β5-1 and β5-2 HEY cells. Black histogram is secondary antibody only. C, mean adherent HEY growth over 4 days (+/− SD, * $p<0.05$). D, Mean Scr, β5-1 and β5-2 HEY soft agar colony growth over 7 days (+/− SD, * $p<0.05$, *** $p<0.001$). E, representative spheroid fluorescent staining for pY397 FAK (red), OPN

(green), and cell nuclei (blue) of Scr and β5-1 shRNA HEY cells. Scale is 50 μm. F, orthotopic tumor growth of Scr (n=7), β5-1 (n=9), and β5-2 (n=10) HEY cells in the ovarian bursa. Values are mean tumor mass after 21 days (+/− SD, * $p<0.05$, ** $p<0.01$). G, serum from Scr and β5-1 HEY tumor-bearing mice was analyzed by anti-hOPN immunoblotting. Densitometry was used to determine mean values (n=7 tumors each, +/− SD, * $p<0.05$).

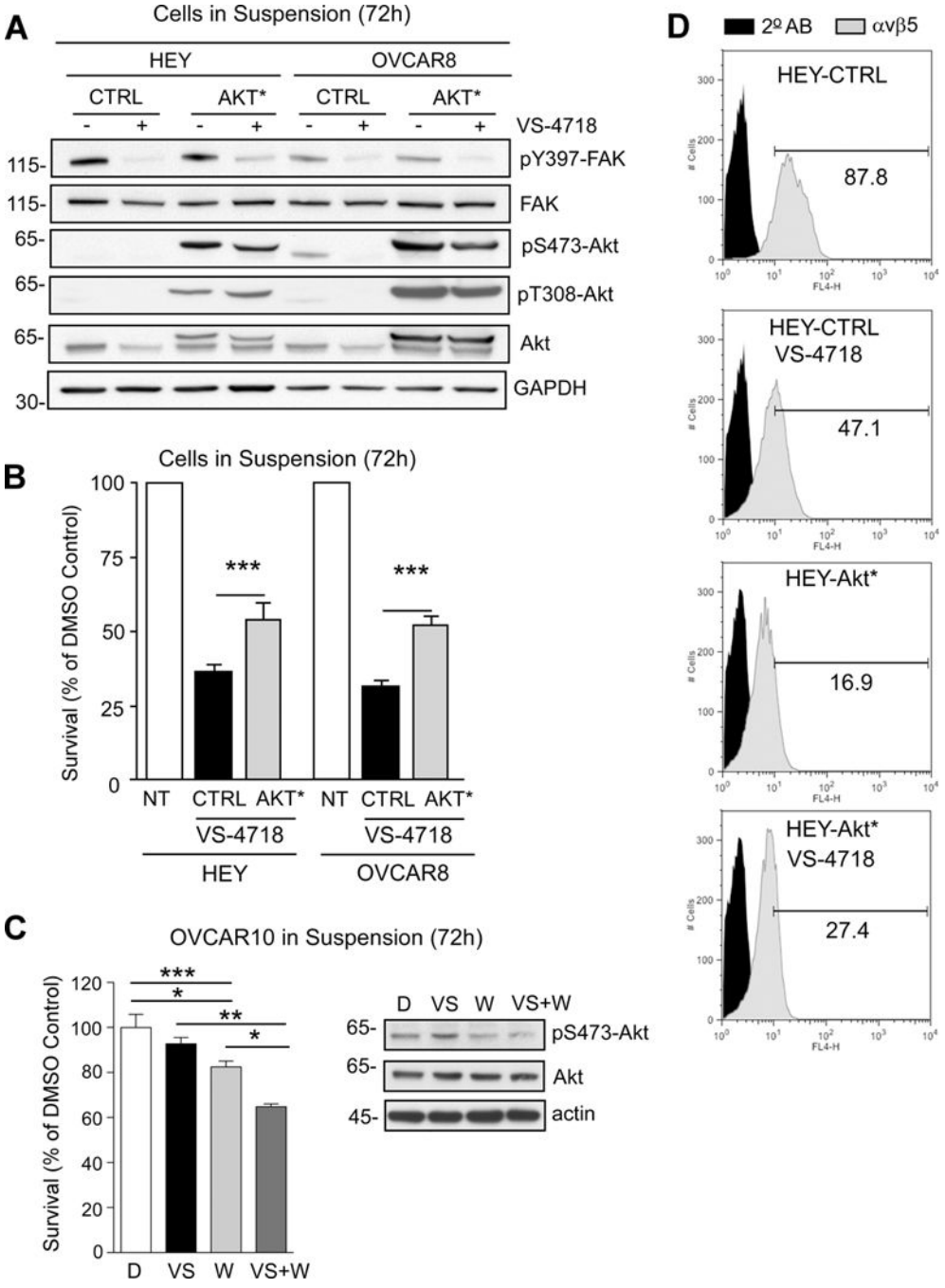

Figure 6.

Stable activated-Akt (Akt*) expression in HEY and OVCAR8 cells promotes anchorage-independent growth and β5 integrin surface expression in the presence of VS-4718. A, immunoblotting for pY397 FAK, FAK, pS473 Akt, pT308 Akt, Akt, and GAPDH in control vector (CTRL) or Akt*-expressing HEY or OVCAR8 cells cultured in suspension for 72 h with 1 μM VS-4718 as indicated. B, HEY and OVCAR8 non-transfected (NT), CTRL-, and Akt*-expressing cells were evaluated for anchorage-independent growth over 72 h in DMSO or 1 μM VS-4718. C, OVCAR10 cells plated in suspension for 72h and treated with

DMSO (D), 0.1 μM VS-4718 (VS), or 0.1 μM Wortmannin (W) alone or in combination. Right, immunoblotting for pS473 Akt, Akt, and actin. B and C, values are means (+/− SEM) of triplicate points from three independent experiments (* $p<0.05$, ** $p<0.01$, *** $p<0.001$). D, flow cytometry of αvβ5 surface expression in CTRL or Akt* HEY cells cultured in DMSO or 1 μM VS-4718 for 72 h. Dark histogram is secondary antibody only.